Boundary Control of a Bipolar Square-Wave Generator Using Second-Order Switching Surface

Kelvin K.S. Leung, Julian Y.C. Chiu, and Henry S.H. Chung
Department of Electronic Engineering
City University of Hong Kong
Tat Chee Avenue, Kowloon Tong, Kowloon, Hong Kong
e-mail: eeshc@cityu.edu.hk

***Abstract* - This paper presents a boundary control of bipolar square-wave generator using a second-order switching surface. The switching surface is derived by estimating the state trajectory movement after a switching action, resulting in a high state trajectory velocity along the switching surface. This phenomenon accelerates the trajectory moving towards the target operating point. A near-optimum performance can be achieved after a large-signal disturbance or output reference variation. The theory is verified with both simulation and experimental results.**

***Index Terms* - Boundary control, dc/ac inverter, first-order switching surface, second-order switching surface.**

I. INTRODUCTION

Switching converters are an important class of systems that operate by variable structure control. Boundary control is a geometric based control method suitable for those switching converters having time-varying circuit topology. Based on the large-signal trajectories of the converter on the state plane, a switching surface is defined to dictate the switching actions. An ideal switching surface can achieve global stability, good large-signal operation, and fast dynamics. State trajectory control technique [1, 2] can achieve steady-state operation for a step change in input voltage or output current in one on/off control by selecting suitable switching surface as the control function, but the control requires either sophisticated digital processor or analog computation.

Due to the complexity of the original state trajectory control, R. Redl and N.O. Sokal [3] proposed using feed-forward of output current and input voltage with current-mode control to achieve near-optimum dynamics performance of switching-mode power supplies.

By combining sliding-mode technique and optimal control theory, the optimal control law for minimum transient time is proposed in [4] and [5]. This method provides time-optimal output regulation without overshoot; however, approximations procedure is required for practical implementation of the control.

By approximating the ideal switching surface with a second-order function, second-order switching surface control can achieve near-optimum large-signal response with simple implementation of the control circuit [6]. In this paper, this control concept will be applied to control the bipolar square-wave generator. In Section II, the basic operation principle is depicted. Various simulations and experiments have been done and shown in Section III to verify the proposed method. Finally, conclusions are summarized in section IV.

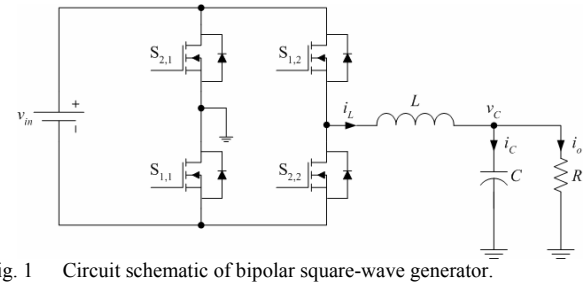

Fig. 1 Circuit schematic of bipolar square-wave generator.

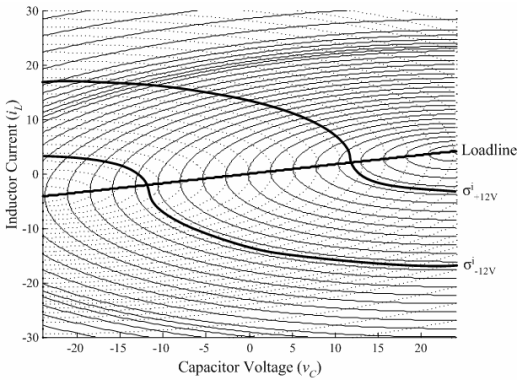

Fig. 2 Positive- and negative-state trajectories of the bipolar square wave generator.

II. PRINCIPLE OF OPERATION

Fig. 1 shows the circuit schematic of the bipolar square wave generator. The converter dynamics can be expressed by the state-space equation of

$$\dot{x} = A_0 x + B_0 u + (A_1 x + B_1 u) q_1 + (A_2 x + B_2 u) q_2 \quad (1)$$

where $x = [i_L \quad v_C]$, A_1 and B_1 are constant matrix and q_i represents the state of the switch $S_{i,n}$. $S_{i,n}$ is on if $q_i = 1$, and

The work described in this paper was fully supported by a grant from CityU (Project No. 7001595).

is off is $q_i = 0$. Matrices A_0, B_0, A_1, B_1, A_2, and B_2 are defined as $A_0 = \begin{bmatrix} 0 & -\frac{1}{L} \\ \frac{1}{C} & -\frac{1}{RC} \end{bmatrix}$, $B_0 = \begin{bmatrix} 0 \\ 0 \end{bmatrix}$, $A_1 = \begin{bmatrix} 0 & 0 \\ 0 & 0 \end{bmatrix}$, $B_1 = \begin{bmatrix} \frac{1}{L} \\ 0 \end{bmatrix}$, $A_2 = \begin{bmatrix} 0 & 0 \\ 0 & 0 \end{bmatrix}$, $B_2 = \begin{bmatrix} -\frac{1}{L} \\ 0 \end{bmatrix}$.

A family of the on- and off-state trajectories, as well as the load line, is shown in Fig. 2. They are obtained by solving (1) with different initial conditions when $R = 5.76\Omega$. The component values used in the analysis are tabulated in Table I. The positive-state trajectory is obtained by setting $\{q_1, q_2\} = \{1, 0\}$, while the negative-state trajectory is obtained by setting $\{q_1, q_2\} = \{0, 1\}$. As discussed in [1], the tangential component of the state-trajectory velocity on the switching surface determines the rate at which successor points approach or recede from the target operating point. An ideal switching surface σ^i that gives fast dynamics should be on the only trajectory passing through the target operating point. σ^i for target operating point at 12V and -12V are shown in Fig. 2. Although σ^i can achieve steady-state operation for a step change in output current or reference voltage in one on/off control, the control requires sophisticated computation for solving the only positive-state and negative-state trajectory that passes the target operating point and it is load-dependent. A second-order surface σ^2, which is near to the ideal surface around the operating point, is derived in the following. The concept is based on estimating the state trajectory after a hypothesized switching action. Criteria for switching $S_{i,n}$ are given as below.

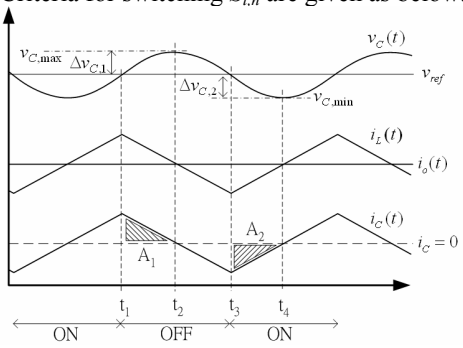

Fig. 3 Typical waveforms of v_C, i_L, i_o and i_C.

A. Criteria for switching off $S_{1,n}$ and switching on $S_{2,n}$

Fig. 3 shows the typical waveforms of v_C and i_C. $S_{1,n}$ is originally in on state and is switching off at the hypothesized time instant t_1. The objective is to determine t_1, so that v_C is equal to $v_{C,\max}$ at t_2 (at which $i_C = 0$). Thus,

$$i_C = C\frac{dv_C}{dt} \tag{2}$$

$$-(v_{in} + v_o) = L\frac{di_L}{dt} \tag{3}$$

By using $i_L = i_C + i_o$ and assuming i_o to be constant,

$$\frac{di_C}{dt} = \frac{di_L}{dt} \approx -\frac{v_{in} + v_o}{L}$$

$$dt \approx -\frac{L}{v_{in} + v_o} di_C \tag{4}$$

Based on (2),

$$\Delta v_{C,1} = v_C(t_2) - v_C(t_1) = v_{C,\max} - v_C(t_1) = \frac{1}{C}\int_{t_1}^{t_2} i_C dt \tag{5}$$

By substituting (4) and $i_C(t_2) = 0$ into $\frac{1}{C}\int_{t_1}^{t_2} i_C dt$, eq. (5) can be derived. In order to ensure that v_C will not go above $v_{C,\max}$, $S_{1,n}$ should be switched off and $S_{2,n}$ be switched on when

$$v_C(t_1) = v_{C,\max} - \frac{1}{2}\frac{L\, i_C{}^2(t_1)}{C(v_{in} + v_o)} = v_{C,\max} - k_1(v_{in}, v_o)\, i_C{}^2(t_1) \tag{6}$$

and

$$i_C(t_1) > 0 \tag{7}$$

B. Criteria for switching on $S_{1,n}$ and switching off $S_{2,n}$

As shown in Fig. 3, $S_{1,n}$ is originally in off state and is switched off at the hypothesized time instant t_3. The objective is to determine t_3, so that v_C is equal to $v_{C,\min}$ at t_4 (at which $i_C = 0$). Thus,

$$i_C = C\frac{dv_C}{dt} \tag{8}$$

$$v_{in} - v_o = L\frac{di_L}{dt} \tag{9}$$

By using $i_L = i_C + i_o$ and assuming i_o to be constant,

$$dt \approx \frac{L}{v_{in} - v_o} di_C \tag{10}$$

Based on (8),

$$\Delta v_{C,2} = v_C(t_4) - v_C(t_3) = v_{C,\min} - v_C(t_3) = \frac{1}{C}\int_{t_3}^{t_4} i_C dt \tag{11}$$

By substituting (10) and $i_C(t_4) = 0$ into $\frac{1}{C}\int_{t_3}^{t_4} i_C dt$, eq.(11) can be expressed to ensure that v_C will not go below $v_{C,\min}$, $S_{1,n}$ should be switched on and $S_{2,n}$ be switched off when

$$v_C(t_3) = v_{C,\min} + \frac{1}{2}\frac{L\, i_C{}^2(t_1)}{C(v_{in} - v_o)} = v_{C,\min} + k_2(v_{in}, v_o)\, i_C{}^2(t_3) \tag{12}$$

and

$$i_C(t_3) < 0 \tag{13}$$

Based on (6), (7), (12), (13) and $v_{C,\min} = v_{C,\max} = v_{ref}$, the following σ^2 can be concluded,

$$\sigma^2(i_L, v_C) = \begin{cases} k_1\,(i_L - \frac{v_C}{R})^2 + (v_C - v_{ref}), & (i_L - \frac{v_C}{R}) > 0 \\ -k_2\,(i_L - \frac{v_C}{R})^2 + (v_C - v_{ref}), & (i_L - \frac{v_C}{R}) < 0 \end{cases} \tag{14}$$

The equation can be further written into a single expression of

$$\sigma^2(i_L, v_C) = c_2 (i_L - \frac{v_C}{R})^2 + (v_C - v_{ref}) \qquad (15)$$

where $c_2 = \frac{1}{2} k_1 \left(1 + \text{sgn}(i_L - \frac{v_C}{R})\right) - \frac{1}{2} k_2 \left(1 - \text{sgn}(i_L - \frac{v_C}{R})\right)$

σ^2 consists of a second-order term and is close to σ^i near the operating point. However, discrepancies occur, when the state is far from the operating point because of the approximations in (4) and (10). Fig. 5 shows the controller implementation. The control circuit can be implemented by using simple analog devices. A multiplier is required to compute the function of k_1, k_2 and squaring of i_C, the remaining parts is handled by simple logic circuits.

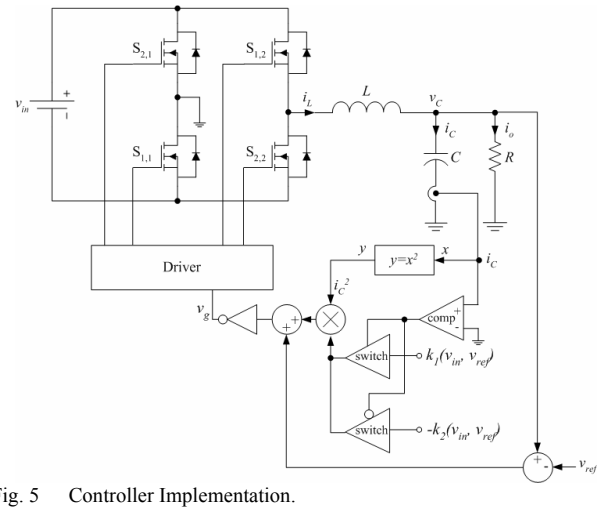

Fig. 5 Controller Implementation.

III. SIMULATION AND EXPERIMENTAL VERIFICATION

A full-bridge inverter with the component values tabulated in Table I is studied. Fig. 6 shows a 24V peak-to-peak square-wave output. The output voltage can revert to it steady state within three switching actions. Compared with the optimum control with σ^i, one extra switching action is required for the voltage to revert to it steady state. σ^2 control is based on the assumption of constant output current during the transient, however, as i_o is not in the steady state during the large signal swing, Δi_L is different from Δi_C. There are discrepancies in predicting the output, however, near-optimum response can still be achieved.

Fig. 7 shows the dynamic behavior of output voltage for 4V, 12V, 28V and 40V peak-to-peak square-wave reference by simulations. Fig. 8 and 9 shows the macroscopic view and microscopic view of the corresponding experimental results. It can be observed that when transient occurs, v_o can follow v_{ref} without overshoots. For larger signal swing, one more switching action may require for v_o reaching it desired value. Fig. 10 shows the transient response to load varying from i_o = 2A (24W) to 9A (108W) and vice versa. The output can revert to the steady state in two switching actions.

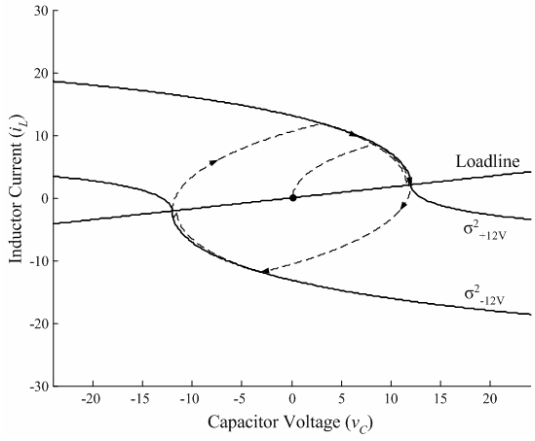

(a)

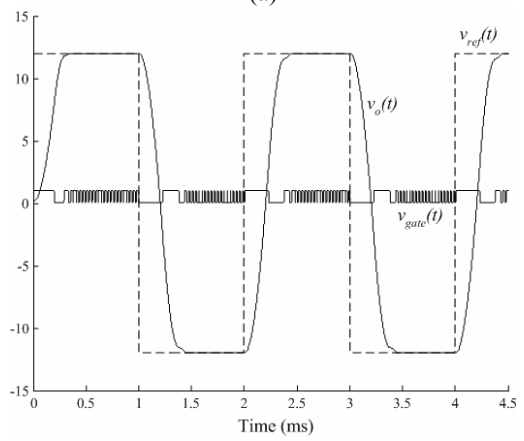

(b)

Fig. 6 Simulated pulsating output voltage and control signal. (a) state-plane. (b) time-domain

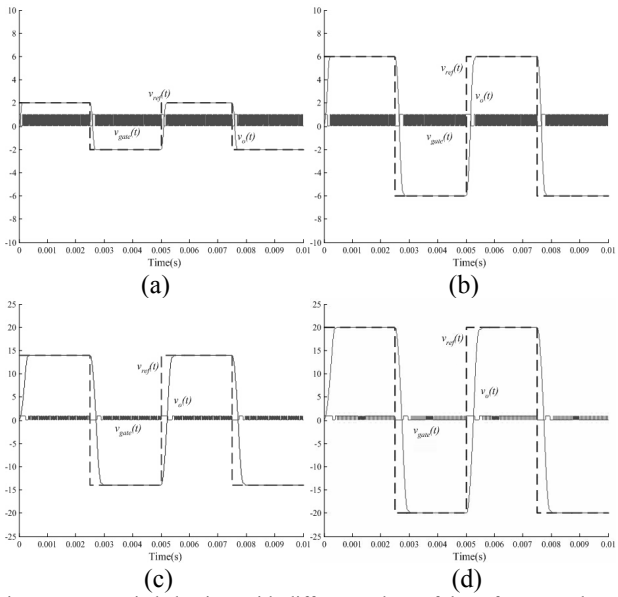

(a) (b) (c) (d)

Fig. 7 Dynamic behaviors with different values of the reference voltage. (a) 4Vp-p. (b) 12Vp-p. (c) 28Vp-p. (d) 40Vp-p.

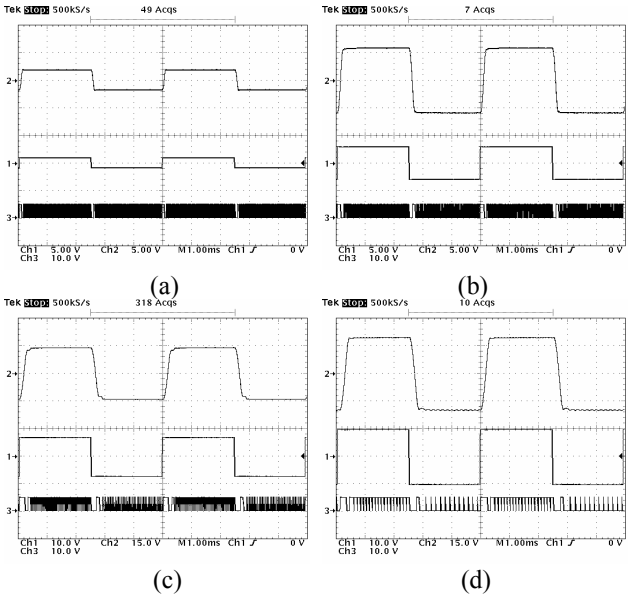

(a) (b) (c) (d)

Fig. 8 Experimental results of dynamic behaviors with different values of reference voltages in macroscopic view. [Ch3: v_{gate} (10V/div)] (a) 4Vp-p. [Ch1: v_{ref} (5V/div), Ch2: v_o (5V/div)] (b) 12Vp-p. (c) 28Vp-p. [Ch1: v_{ref} (10V/div), Ch2: v_o (15V/div)] (d) 40Vp-p.

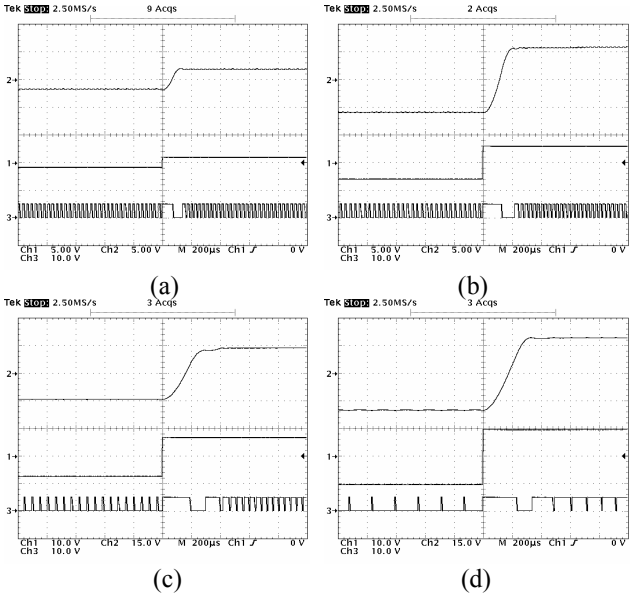

(a) (b) (c) (d)

Fig. 9 Experimental results of dynamic behaviors with different values of the reference voltages in microscopic view. [Ch3: v_{gate} (10V/div)] (a) 4Vp-p. [Ch1: v_{ref} (5V/div), Ch2: v_o (5V/div)] (b) 12Vp-p. (c) 28Vp-p. [Ch1: v_{ref} (10V/div), Ch2: v_o (15V/div)] (d) 40Vp-p.

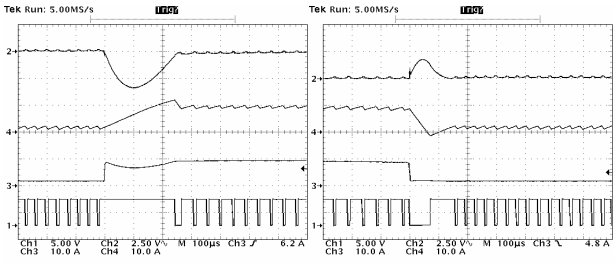

(a) (b)

Fig. 10 Transient response at v_o = 12V. [Ch1: v_{gate} (5V/div), Ch2: v_o (2.5V/div), Ch3: i_o (10A/div), Ch4: i_L (10A/div)]. (a) i_o is changed from 2A (24W) to 9A (108W). (b) i_o is changed from 9A to 2A.

IV. CONCLUSION

A boundary control using the second order switching surface in buck converter for bipolar square-wave generation has been proposed. Near-optimum dynamic performance can be achieved without any sophisticated computation or circuitry. The proposed idea is verified by both simulation and experimental results.

TABLE I. COMPONENTS VALUES

Parameters	Values
v_{in}	24V
L	500μH
C	100μF
v_{ripple}	20mV

REFERENCES

[1] W. Burns, et al, "State trajectories used to observe and control dc-to-dc converters," *IEEE Trans. Aerosp. Electron. Systs.,* vol.12, no.6, pp.706-717, Nov. 1976

[2] W. Burns and T.G. Wilson, "Analytical derivation and evaluation of a state trajectory control law for dc-to-dc converters," in *Proc. Power Electron. Spec. Conf.,* pp.70-85, 1977.

[3] R. Redl and N.O. Sokal, "Near-optimum dynamics performance of switching-mode power converters using feedforward of output current and input voltage with current-mode control", *IEEE Trans. Power Electron.,* vol. 1, no. 3, pp. 181-192, Jul. 1986

[4] D. Biel, L. Martinez, J. Tenor, B. Jammes and J.C. Marpinard, "Optimum dynamic performance of a buck converter". *in Proc.of ISCAS,* 1996, pp.589-592.

[5] D. Biel, L. Martinez, J. Lopez, Y. Perez, B. Jammes and J.C. Marpinard, "Minimum-time control of a buck converter for bipolar square-wave generation", *in Proc. Of European Space Power Conf.,* 1998, pp.345-350.

[6] Kelvin K. S. Leung and Henry S. H. Chung, "Derivation of a Second-Order Switching Surface in the Boundary Control of Buck Converters", *IEEE Power Electronics Letters*, Vol.2, No. 2, June 2004, pp.63-67.